Indian Journal of Pure & Applied Physics
Vol. 52, August 2014, pp. 525-530

Band gap properties in two-dimensional phononic crystal slabs with neck structures

Kunpeng Yu, Tianning Chen*, Xiaopeng Wang & Chao Zhang

School of Mechanical Engineering & State Key Laboratory for Strength and Vibration of Mechanical Structures, Xi'an Jiaotong University, Xi'an 710049, China

*E-mail: tnchen229@126.com

Received 29 May 2013; revised 20 January 2014; accepted 19 March 2014

The numerical investigation on elastic wave band gap properties in two-dimensional phononic crystal slabs composed of periodic cylinders inserted in a homogeneous slab is presented. The cylinders are not connected with the slab directly but linked it through some neck structures constituted by part of an annular cylinder. By using the finite element method, the band structures of the phononic crystal are analyzed and the geometric parameters of the structure are studied for their effects on the band gap properties. Results show that band gaps with low frequencies appear in this structure. The largest band gap can be influenced significantly by the geometric parameters of the neck (including the length, the position, the central angle and the rotation angle of the neck). Furthermore, the vibration eigenmodes of the structure are calculated to reveal the relationship between band gaps and the geometry of the structure. Results show that the occurrence of low frequency band gaps are attributed to the coupling effect of swing modes of cylinders and the plate wave modes of the slab matrix.

Keywords: Phononic crystal slab, Band gap, Finite element method, Neck

1 Introduction

In the past years, a new class of functional composites, the phononic crystals (PCs), has received a lot of interest due to their novel physical properties and wide range of potential applications[1-8]. PCs are artificial media constituted by a periodical repetition of inclusions arranged with various topologies in some different host materials[9-11]. The interest in these media arises mainly from their possibility of exhibiting absolute phononic band gaps (PBGs), i.e., frequencies within which the propagation of acoustic or elastic waves is forbidden in all directions. This surprising property leads the PCs to several potential applications such as the design of new acoustic devices, noise reduction and vibration isolation in high-precision mechanical systems[12-15]. Consequently, the study on the PCs has become one of the most attractive areas in physics, acoustics and engineering.

To meet the needs of PCs in various fields of application, the proposal of novel PC structures that can yield PBGs in required frequency ranges and the investigations on the band gap properties are of great importance. In the early years, a lot of researches were carried out to design new PCs and study the influencing factors of the band gaps[16-21]. Liu *et al*[22] presented a three-component localized resonance PC structure constituted by periodic hard cores coated with soft material in host material structure. Results show that this structure could exhibit band gaps two orders of magnitude smaller than the relevant wavelength. As the localized resonance mechanism (LR) breaks the restriction of the Bragg mechanism on the relationship between the lattice constant and the wavelength, it insinuates the LRPCs greater value in the practical application fields. Thus, more and more researches were focused[23-28]on the LRPCs. All the novel PCs mentioned above are composed of periodic localized resonators placed on the matrix, worked as the spring-mass systems. Recently, a two-dimensional PC structure composed of periodic cylinders embedded in a homogenous matrix where the cylinders are not connected with the matrix directly but through the neck structures is presented[29]. The authors investigated the band properties of the structure and the influencing factors of the gaps. However, the proposed PC in the present paper is assumed to be infinite in the *z*-direction. The band gap properties of the PC with finite thickness in the z-direction have not been reported yet. In fact, when the thickness of the structure is finite, the PC becomes a two-dimensional slab and there may be more geometrical parameters to modulate the band gaps,

which will be very significant for the practical application of the PCs. Therefore, studies on PC slabs with neck structures will be more interesting.

In the present paper, a novel two-dimensional PC slab composed of periodic cylinder inclusions embedded in a homogenous matrix is numerically investigated. The cylinder inclusions are not connected directly with the matrix but linked through some neck structures constituted by part of an annular cylinder. The band gap properties of the PC slab are studied and the effects of the geometrical parameters on the gap modulation are analyzed in detail.

2 Model and Method

As shown in Fig. 1(a), the PC structure considered here is a slab with an array of cylinder inclusions inserted in it. The cylinder inclusions are not contacted with the slab matrix directly but through some neck structures constituted by part of an annular cylinder. The thickness of the whole structure along the *z*-direction is *h* and the lattice constant along the *x*- and *y*-directions is *a*. In Fig. 1(b), r_1 is the outer radius of the neck, and r_2 is the inner radius of the neck meanwhile the radius of the cylinder inclusions. The central angle θ represents the arc length of the neck, and the rotation angle β, the angle between the centerline of the neck and the *x*-axis, describes the position of the neck in the vacuum ring between the matrix and the cylinder inclusion. In Fig. 1(c), *L* is the length of the neck structure and *s* is the displacement of the neck from the middle cross- section of the slab matrix along the *z*-direction. The whole PC unit cell is surrounded by vacuum and extends repeatedly along the *x*- and *y*-directions.

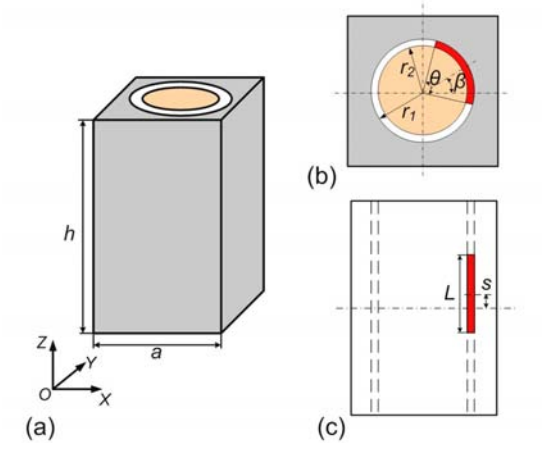

Fig. 1 — Schematic view of the unit cell of the PC slab with neck structures (a) the main view (b) the top view and (c) the cutaway view along the *xz*-plane

In order to investigate the band gap properties of the proposed PC slabs, a series of calculations on the dispersion relations and displacement fields of eigenmodes are conducted with the finite-element method (FEM) based on the Bloch theory[29,30]. For the propagation of the elastic waves in solid systems, the governing equations are given as follows:

$$\sum_{j=1}^{3}\frac{\partial}{\partial x_j}\left(\sum_{l=1}^{3}\sum_{k=1}^{3}c_{ijkl}\frac{\partial u_k}{\partial x_l}\right)=\rho\frac{\partial^2 u_i}{\partial t^2}\quad (i=1,2,3) \qquad \ldots(1)$$

where ρ is the mass density, c_{ijkl} the elastic constants, *t* the time, *u* is the displacement field and x_j (j = 1, 2, 3) represent the coordinate variables *x*, y and z, respectively. According to the Bloch theory, the displacement field in periodic solid system can be expressed as:

$$\mathbf{u}(\mathbf{r})=\exp\left|i(\mathbf{k}\cdot\mathbf{r})\right|\mathbf{u}_{\mathbf{k}}(\mathbf{r}), \qquad \ldots(2)$$

where $\mathbf{k}$ = (k_x, k_y) is the wave vector, $\mathbf{u_k}(\mathbf{r})$ is a periodical vector function with the same periodicity as the crystal lattice. Based on Eq. (2), only the unit cell in Fig. 1(a) needs to be considered during the calculations of the dispersion relations since the infinite system is periodic along the *x*- and *y*-directions simultaneously. With the FEM, Bloch periodic boundaries are adopted on the two group boundaries in *xy*-plane, written as:

$$\mathbf{U}(\mathbf{r}+\mathbf{a})=\exp\left|i(\mathbf{k}\cdot\mathbf{r})\right|\mathbf{U}(\mathbf{r}), \qquad \ldots(3)$$

where $\mathbf{U}$ is the displacement at the nodes, *r* the position vector located at the nodes and $\mathbf{a}$ is the vector that generates the point lattice associated with the PCs. The Bloch wave vector $\mathbf{k}$, delimited in the first Brillouin zone of the reciprocal lattice, is adopted to describe the related phase relation of a plane wave on the boundaries. By varying the value of $\mathbf{k}$ in the irreducible Brillouin zone and solving the eigenvalue problems generated by the FEM algorithm, the dispersion relations (i.e., the band structures) as well as the displacement fields of eigenmode can be obtained.

3 Results and Discussion

3.1 Result of band structure calculation

Figure 2 shows the calculated dispersion relations for the proposed PC slab composed of periodic steel cylinders inserted in the epoxy matrix with steel neck

structures. The materials applied in the calculations are steel for necks and cylinder inclusions, and rubber for the slab matrix, respectively. The elastic parameters for them are chosen as follows: the Young's modulus E = 2 GPa, Poisson's ratio v = 0.4 and ρ = 1300 kg/m^3 for rubber; E = 200 GPa, Poisson's ratio v = 0.33 and ρ = 7850 kg/m^3 for steel. Meanwhile, the following geometrical parameters are adopted: r_o = 15 mm, r_i = 14 mm, θ = 90°, β = 0°, a = 34 mm, h = 20 mm, L = 20 mm and s =0 mm. The filling factor γ = 61.12%. It is observed from Fig. 2 that 11 bands exist in the band structure in the frequency range 0-5 kHz, where three complete band gaps are involved. The first band gap locates between the sixth and seventh band, extending from 2.48 to 3.61 kHz. The gap width and relative gap width are 1.13 kHz and 37.11%, respectively. The second gap locates between the seventh and eighth band and that of the third one is between the ninth and tenth band, and their gap widths are much smaller than the first gap. The gap width for the second gap is 97 Hz (4.08-4.177 kHz) and for the third one is 85 Hz (4.535-4.620 kHz), respectively. Besides, there are two incomplete band gaps in the ΓX direction. The first one ranges from 0.85 to 0.975 kHz, with the gap width 0.125 kHz, and the second one ranges from 1.06 to 3.75 kHz with the gap width 2.69 kHz.

From the calculation on the band structure of the PC slab, it can be seen that the proposed structure can yield relative large band gaps in low frequency ranges, inferring this type of PC beneficial for engineering applications such as the vibration isolation and the provision of no-vibration processing environment in high-precision mechanical systems. In the following, the geometrical parameters of the PC structure are investigated for their effects on the band gap modulations. As the first band gap is the largest one, it is more worthy of being studied. So the analysis is mainly focused on the first band gap.

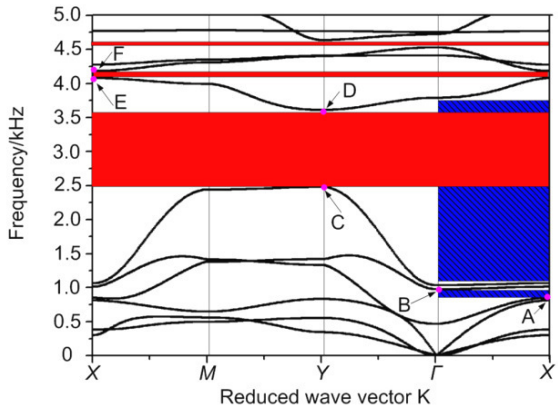

Fig. 2 — Band structure of the PC structure modeled in Fig. 1

3.2 Effects of the geometrical parameters of the neck structure

From Fig. 1 it can be seen that the geometrical parameters of the neck structure mainly include the central angle θ, the rotation angle β, the neck length L and the neck displacement along the z-direction s. These parameters are sequentially studied for their effects on the first band gap. During all these calculations, the r_o = 15 mm, r_i = 14 mm and a = 34 mm remain unchanged.

Firstly, keeping β = 0°, L = 50 mm and s = 0 mm, the influence of the central angle θ of the neck on the band gap is investigated. Figure 3 shows the evolution of the band gap as a function of the central angle parameter. The central angle varies from 60 to 300°. It can be observed that, with the increase of the central angle, both the lower edge (black line with cross points) and upper edge (red line with circle points) move to a higher frequency range. With the increase of the central angle θ from 60 to 300°, the lower edge raises from 2.13 to 5.025 kHz, and the upper edge raises from 2.883 to 8.524 kHz. When θ is small, for example smaller than 200°, since the increasing ratios of the upper edge and lower edge are very similar with each other, the gap width of the first band gap remains almost unchanged. When θ is large enough, as the rate of increase of the lower edge trends to be flatten while that of the upper edge becomes faster, the gap width increases accordingly.

Secondly, keeping θ = 90°, L= 50 mm and s = 0 mm, the effect of the rotation angle on the band gap is investigated. Figure 4 shows the evolution of

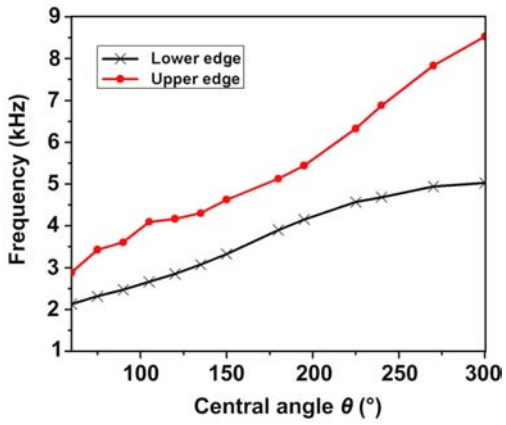

Fig. 3 — Evolution of the band gap as a function of the central angle θ with β = 0°, L = 50 mm and s = 0 mm

the band gap as a function of the rotation angle parameter. It can be seen that, with the increasing of the neck rotating from 0 to 45°, the lower edge of the band gap moves to the lower frequencies, i.e., from 2.492 to 1.961 kHz, while the upper edge raises from 3.712 to 3.974 kHz. The gap width parameter modulated is considerable large, which is from 1.22 to 2.013 kHz. When the angle still increases from 45 to 90°, it can be observed that the lower edge rises and the upper decreases. Obviously, the figure is symmetrical with the vertical line corresponding to $\beta = 45°$ as the axis of symmetry.

Thirdly, keeping $\theta = 90°$, $\beta = 0°$ and $s = 0$ mm, the effect of the neck length on the band gap is investigated. Figure 5 shows the evolution of the band gap as a function of the neck length parameter. One premise should be noted, the increase of the neck length is implemented by extending it on both directions of z-axis at the same time. From Fig. 5, it

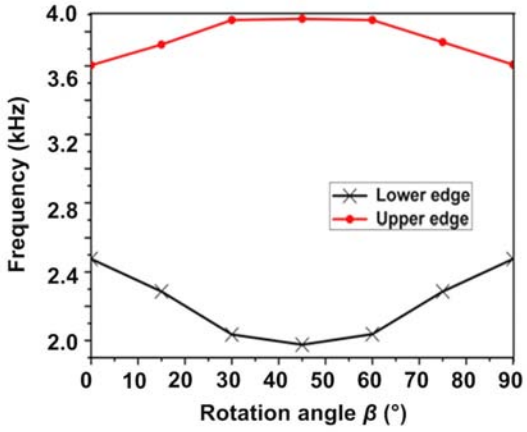

Fig. 4 — Evolution of the band gap as a function of the rotation angle β with $\theta = 90°$, $L = 50$ mm and $s = 0$ mm

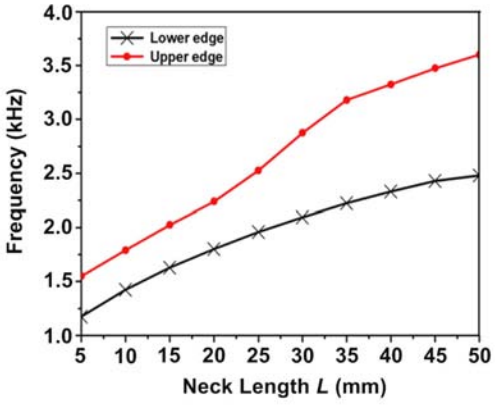

Fig. 5 — Evolution of the band gap as a function of the rotation angle L with $\theta = 90°$, $\beta = 0°$ and $s = 0$ mm.

can be seen that the effects of the neck length on both edges of the gap are very similar with that of the central angle (seen in Fig. 3). With the increasing of the neck length, both the upper and lower edges of the gap rise. However, the amplitude of increase that this parameter modulates is much smaller than the central angle does, as the lower edge raises from 1.18 to 2.48 kHz while the upper edge from 1.55 to 3.61 kHz. It can be concluded that, although this parameter cannot modulate the gap width significantly, it lowers the starting frequency of band gap to some extent, which is beneficial for broadening the application of PC in lower frequencies.

Finally, keeping $\theta = 90°$, $\beta = 0°$ and $L = 10$ mm, the effect of the neck displacements along the z-direction s on the band structure is investigated. The results are shown in Fig. 6. Four groups of neck displacement are chosen for the calculations: (a) $s = 0$ mm, (b) $s = 5$ mm, (c) $s = 10$ mm and (d) $s = 15$ mm. From Fig. 6(a), it can be observed that, ten bands exist in the band structure in the frequency range 0-2.5 kHz where one complete gap and one incomplete gap are involved. The gaps located between the sixth and seven bands, extending from 1.436 to 1.761 kHz and 0.68 to 1.436 kHz, respectively. When the neck displacement increases to $s = 5$ mm, as shown in Fig. 5(b), some points on the bands upon the complete gap (*MY* direction) decreases, resulting in the shrinking of the gap. As the six bands below the complete gap change are small, the original incomplete gap remains almost unchanged. Further

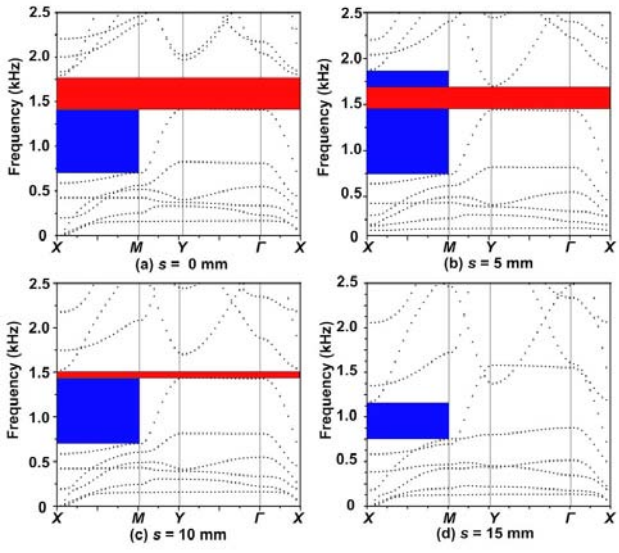

Fig. 6 — Band structures with different neck displacements along the z-direction s, with $\theta = 90°$, $\beta = 0°$ and $L = 10$ mm

shift the neck to s = 10 mm, it can be observed from Fig. 6(c) that the eigenfrequencies of the seventh bands along the *XM* direction decline significantly, more than that of eigenfrequencies along the *XM* direction do, causing the complete gap to further shrink. Still the incomplete gap remains unchanged as the six bands below the complete gap arise no major changes. When the neck displacement increases to s = 15 mm, the complete gap disappears and the incomplete gap shrinks. From the analysis above, it can be concluded that the neck displacement parameter mainly influences the bands at high orders while yields little impact on bands at low orders.

3.3 Displacement fields of eigenmodes

To better understand the relationship between the neck structure and the band gap modulations, the displacement fields of eigenmodes of the PC structure are calculated. The results are shown in Fig. 7. The colour map denotes the magnitude of the total displacement vector field. In Fig. 7, mode A belongs to the fourth band, B to the fifth, C to the sixth and D to the seventh, respectively. From Fig. 7(a) it can be seen that, mode A is mainly the oscillation of the cylinder inclusion in the *xz*-plane. As the slab matrix is connected with the cylinder through the neck, the matrix on the upper right is extruded and the lower right compressed. Similarly, the vibration of mode B is mainly concentrated at the swing of the cylinder inclusion along the *yz*-plane. Accordingly, shearing vibration occurs on the upper and lower slab layers of the matrix. Unlike mode A and B, mode C is mainly the torsional vibration of the cylinder inclusion, and meanwhile causes the slab matrix rotation through the neck structure. As this mode corresponds to the lower edge of the first band gap, structure changes related with it will influence the gap properties. For the central angle and the neck length parameters, the increase of the parameters will add the contact area of the neck and the slab matrix, therefore increase of the torsional stiffness of the system, and thus raise the lower edge of the band gap. For the rotation angle parameter, it can be seen from Fig. 1(a) that both ends of the neck locate at the corners of the square unit cell where much material gathers. In this case, the torsion of the slab matrix that driven by the neck is difficult. When β = 45°, the neck is rotated to a corner and both ends of it locate at the middle of the side. As material at the neck ends is less, the torsion becomes easy and the eigenfrequency of the structure declines. For the neck displacement parameter, since the modes A, B and C are mainly the vibration of the cylinder and spread to the slab matrix through the neck, the variation of the neck displacement yields little effect on the lower order bands as the contact area and torsional stiffness seldom change. From the Fig. 7(d) it can be found that, mode D, which corresponds to the upper edge of the band gap, is mainly the shearing vibration of the slab matrix along the *z*-direction, and the cylinder and neck remain almost stationary during the process. The increase of the central angle, the rotation angle and the neck length will make the shearing become difficult and accordingly increase the eigenfrequency of the gap edge, causing the upper edge of the gap rises, as shown in Figs 3-5. For the neck displacement parameter, as the neck moves up from the middle of the slab to the surface, the decrease of symmetry weakens the constraint on the shearing vibration, resulting in the upper edge moves to the lower frequencies.

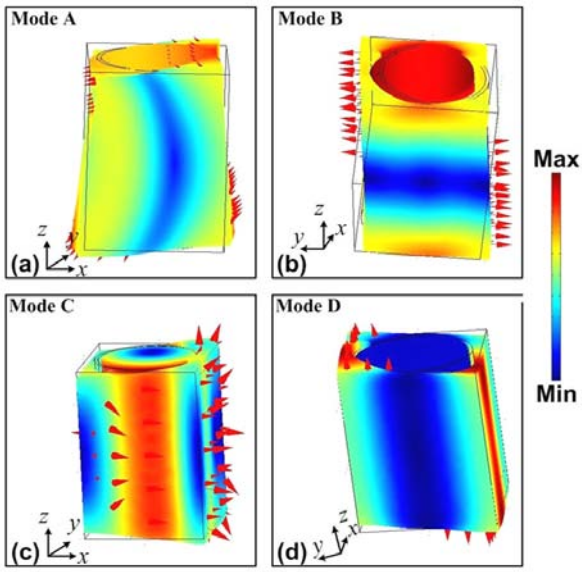

Fig. 7 — Eigenmode shapes and displacement vector fields of the modes marked in Fig. 2: (a) mode A; (b) mode B; (c) mode C; (d) mode D

4 Conclusions

In the present paper, a novel two-dimensional phononic crystal slab composed of periodic cylinders inserted in a homogeneous slab is reported and the band gap properties are investigated numerically by using the FEM. The cylinders are not connected with the slab directly but linked it through some neck structures constituted by part of an annular cylinder. Numerical results show that band gaps with low

frequencies are observed in this PC structure. Geometrical parameters of the neck structure such as the central angle, the rotation angle, the neck length and the neck displacement are studied for their effects on the first large band gap. Results show that the location and gap width of the band gap can be modulated significantly by these geometrical parameters. The increase of the central angle and the neck length raise both the lower and upper edges of the gap and meanwhile enlarge the gap width. The increase of the rotation angle raises the upper edge while declines the lower edge to some extent. However, the increase of the neck displacement declines the upper edge and shrinks the gap width. Moreover, the analysis on the displacement fields of eigenmodes show that these parameters work on the band gap by changing the stiffness of the system. The study in this paper may be valuable to the design of tuning band gaps and isolators in the low-frequency range.

Acknowledgement

The authors gratefully acknowledge financial support from the National Basic Research Program of China under Grant No. 2011CB610306, the Project of National Natural Science Foundation of China under Grant No. 51275377, and the Program for Changjiang Scholars and Innovative Research Team in University under Grant No. IRT1172.

References

1 Vasseur J O, *et al.*, *Phys Rev Lett*, 86 (2001) 3012.
2 Goffaux C & Sánchez-Dehesa J, *Phys Rev B*, 67 (2003) 144301.
3 Yu D, *et al.*, *Phys Lett A*, 376 (2012) 626.
4 Goffaux C & Vigneron J P, *Phys Rev B*, 64 (2001) 075118.
5 Chen A L & Wang Y S, *Physica B*, 392 (2007) 369.
6 Pennec Y, *et al.*, *Appl Phys Lett*, 87 (2005) 261912.
7 Wu M L, Wu L Y, Yang W P & Chen L W, *Smart Mater Struct*, 18 (2009) 115013.
8 Lin S C S, Huang T J, Sun J H & Wu T T, *Phys Rev B*, 79 (2009) 094302.
9 Wang G, Wen J H, Liu Y & Wen X, *Phys Rev B*, 69 (2004) 184302.
10 Khelif A, Djafari-Rouhani B, Vasseur J O & Deymier P A, *Phys Rev B*, 68 (2003) 024302.
11 Sainidou R, Djafari-Rouhani B, Pennec Y & Vasseur J O, *Phys Rev B*, 73 (2006) 024302.
12 Torrent D & Sánchez-Dehesa J, *New J Phys*, 9 (2007) 323.
13 Assouar M B & Oudich M, *Appl Phys Lett*, 99 (2011) 123505.
14 Farhat M, *et al.*, *Appl Phys Lett*, 96 (2010) 081909.
15 Ho K M, *et al.*, *Appl Phys Lett*, 83 (2003) 5566.
16 Goffaux C, *et al.*, *Phys Rev Lett*, 88 (2002) 225502.
17 Sainidou R, Stefanou N, Psarobas I E & Modinos A, *Comput Phys Commun*, 166 (2005) 197.
18 Soliman Y M, *et al.*, *Appl Phys Lett*, 97 (2010) 139502.
19 Leroy V, *et al.*, *Appl Phys Lett*, 95 (2009) 171904.
20 Li X, *et al.*, *J Phys D Appl Phys*, 36 (2003) L15.
21 Hou Z, *Phys Rev E*, 75 (2007) 026608.
22 Liu Z, *et al.*, *Science*, 289 (2000)1734.
23 Yao Y, Hou Z, Wu F & Zhang X, *Physica B*, 406 (2011) 2249.
24 Hsu J C & Wu T T, *Appl Phys Lett*, 90 (2007) 201904.
25 Pennec Y, *et al.*, *Phys Rev B*, 78 (2008) 104105.
26 Hsu J C, *J Phys D Appl Phys*, 44 (2011) 055401.
27 Zhang H B, Chen J J & Han X, *J Appl Phys*, 112 (2012) 054503.
28 Oudich M, Li Y, Assouar M B & Hou Z, *New J Phys*, 12 (2010) 083049.
29 Yu K, Chen T & Wang X, *J Appl Phys*, 113 (2013) 134901.
30 Wang Y F, Wang Y S & Su X X, *J Appl Phys*, 110 (2011) 113520.